

# Miniatured Ring Slotted Circular Patch GNSS Antenna

Rais Ahmad Sheikh<sup>#\*</sup>, Azremi Abdullah Al-Hadi<sup>#</sup>, Thennarasan Sabapathy<sup>#</sup>, Fong Mun Chun<sup>#</sup>, Hidayath Mirza<sup>\*</sup> and Ping Jack Soh<sup>^</sup>

<sup>#</sup>*Advanced Communication Engineering (ACE) CoE, Faculty of Electronic Engineering Technology, Universiti Malaysia Perlis (UniMAP), Kampus Alam UniMAP Pauh Putra, 02600 Arau, Perlis, Malaysia*

<sup>\*</sup>*Department of Electrical Engineering, College of Engineering, Jazan University 45142 Jazan, Kingdom of Saudi Arabia*

<sup>^</sup>*Centre for Wireless Communication, University of Oulu, Erkki Koiso Kanttilan Katu 3, 90570 Oulu, Finland*

<sup>#\*</sup>[raisahmadlko@gmail.com](mailto:raisahmadlko@gmail.com)

**Abstract** — A compact circularly polarized antenna for the Global Navigation Satellite System L1 band operating at 1575.42 MHz is presented. A circular patch antenna is first designed to operate before being integrated with four ring slots to achieve the circular polarization. The antenna features a bandwidth of 1.96 % in L1, with an axial ratio bandwidth of 0.896 %. The antenna radiates towards 0° with a realized gain of 5.58 dB and an angular beamwidth of 96.6°.

**Index Terms** — circular polarized antennas, compact antennas, slot antennas, Global Navigation Satellite System

## I. INTRODUCTION

Global Navigation Satellite System (GNSS) was introduced in 1970, with full operational capabilities in 1995. This system was then combined with various other positioning systems to be known today as Global Navigation Satellite System (GNSS), which employs different frequency bands [1]. The L1 band is widely used signal for satellite navigation and is employed by most satellite navigation applications, devices and systems worldwide [2]. It is also referred as L1 CA (Coarse Acquisition). Circular polarization (CP) characteristic is one of the important requirements in GNSS antenna design. Apart from GNSS, CP antennas have also been designed for various other applications such as WiFi [3], LTE [3], 5G [4] and RFID [5]. Different types of materials have been also adopted for such antennas, including flexible [6] and non-flexible [7] types.

Among the main challenges in designing CP antennas is in obtaining sufficient axial ratio (AR) bandwidth while maintaining simple and compact structures. Broad AR bandwidths enables the reception of low- elevation satellite signals effectively, hence improving the precision [8]. For example, a low multipath antenna is proposed in [9] for the GNSS application. The antenna featured a diameter  $0.576\lambda_0$  and operates at 1.575 GHz. Next, a square patch wearable antenna using textile substrate working for L1 band is proposed in [10]. Cutting two opposite corners of the square patch results CP for the design, which results in a size of  $0.582\lambda_0 \times 0.493\lambda_0 \times 0.052\lambda_0$ . A CP meandered monopole antenna is presented in [11]. The proposed antenna operates at 1.575 GHz where the CP is achieved using Wilkinson power divider with a bandwidth of 13 MHz. This antenna is sized  $0.431\lambda_0 \times 0.473\lambda_0 \times 0.004\lambda_0$ . Bowtie dipoles and spiral antenna designs are comparatively broader in bandwidth, but at the cost of large size. For instance the antenna presented in

[12] is sized at  $1.89\lambda_0$  (ring diameter) and spiral antenna of size  $0.617\lambda_0 \times 0.467\lambda_0 \times 0.106\lambda_0$  [13].

Another key aspect being focused in GNSS antennas is to design the antenna in a compact form without affecting AR. Several techniques to miniaturize the GNSS antenna includes meandering [3], creating slots on the radiator [14] and incorporating fractal geometry on the patch [15]. In this work, an antenna with ring slots of different radii is proposed to obtain the size reduction. It operates in L1 with a compact form ( $0.341\lambda_0 \times 0.341\lambda_0 \times 0.017\lambda_0$ ). CP radiation is achieved using circular slot rings with different radii on the radiator. The small difference in the radii of the circular slot rings produces two orthogonal modes, which are equal in magnitude but has 90° phase shift. Moreover, the use of ring slots on the circular patch results in a more compact antenna.

The rest of this paper is organized as follows. Section II presents the design concept of the proposed antenna, followed by the results in Section III. Finally, the concluding remarks is provided in Section IV.

## II. ANTENNA DESIGN AND STRUCTURE

The proposed antenna contains a circular patch as the radiator, which is fed directly by the coaxial feeding probe, as presented in Figure 1(a). Rogers RO4003C with a thickness of 3.25 mm is used as the substrate. The relative permittivity of the substrate is 3.38 and the loss tangent is 0.002. To excite two orthogonal electric field waves with equal magnitude but phase quadrature for circular polarization radiation requires the following ring slot radii:  $r1 < r2 < r3 < r4$ . The final optimized values are  $r1 = 4$  mm,  $r2 = 6$  mm,  $r3 = 6.5$  mm and  $r4 = 7$  mm. Coaxial feed probe connected to the patch is located along the 45° angle from  $x$ -axis at  $(x_0, y_0)$ , where both coordinates are equal to 9.5 mm as shown in the Figure 1(b). Figure 1(c) illustrates the radius of the circular patch and the radii of ring slots on it. Radius of the patch,  $R$  enables operation in the L1 band target frequency. The  $R$  is 27.7 mm. Four ring slots with radii of  $r1$ ,  $r2$ ,  $r3$  and  $r4$  are created on the radiator, where  $r1$  and  $r3$  are located at  $(x, y) = (\pm 13.5, 0)$  whereas  $r2$  and  $r4$  are located at  $(0, \pm 16.5)$ . CST Microwave Studio Suite has been used to design, simulate, and optimize the structure. Time domain solver setting with hexahedral mesh type is chosen for the simulations and optimization.

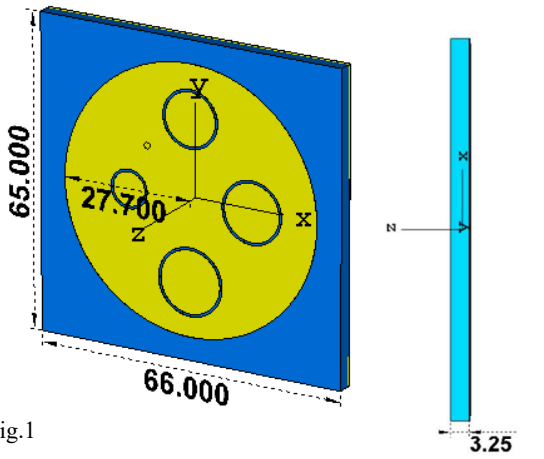
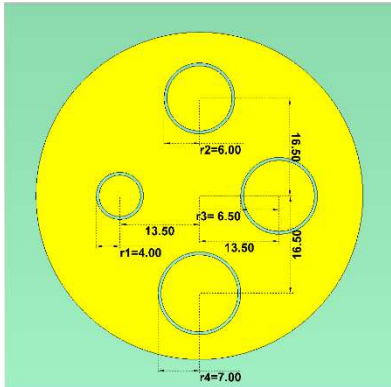


Fig.1

- (a) Perspective view of the proposed design (b) Bottom view of the structure



(c) Radii and separation distance of ring slots

### III. SIMULATED RESULTS

Figure 2 shows the reflection coefficient ( $S_{11}$ ) of the proposed antenna. The antenna resonates at 1575 MHz frequency with  $S_{11}$  of approximately -14 dB, whereas the bandwidth obtained for  $S_{11} < -10$  dB is 30.89 MHz.

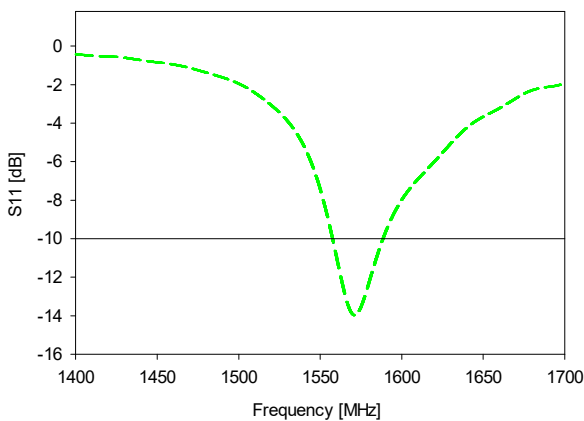


Fig. 2. Reflection coefficients of the proposed antenna

The size of  $R$  heavily influences the antenna reflection coefficient, and a parametric analysis is conducted on this parameter. By changing the  $R$  value from 26.7 mm to 28.7 mm, the corresponding reflection coefficients at higher frequencies and vice versa, as shown in Figure 3.

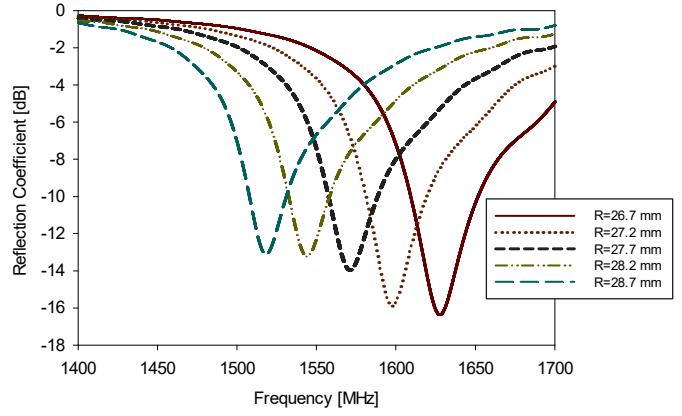


Fig. 3. Radiator radii sweep to achieve impedance matching

Besides that, the depth of the reflection coefficient deteriorates significantly even for small variation in the value of  $R$ . The optimal value for operation at 1575 MHz is found at  $R=27.7$  mm.

On the other hand, ring slots  $r1$  and  $r3$  are located at the distance 13.5 mm from its center to the center of the circular patch, whereas  $r2$  and  $r4$  are at distance  $Y = 16.5$  mm. When changing  $Y$  from 15.5 mm to 18.5 mm, it is found that the axial ratio become lower than 2 dB at 1575 MHz as shown in Figure 4.

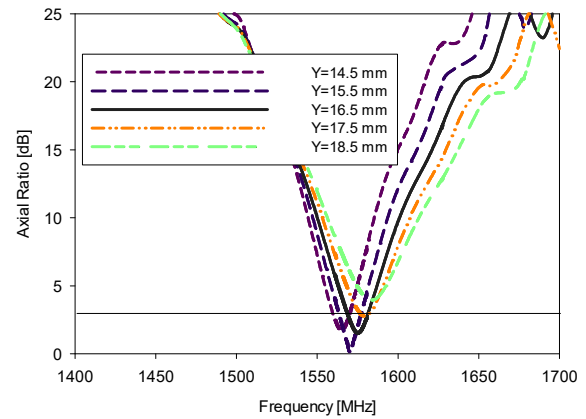


Fig. 4. Separation distance ( $Y$ ) of ring slots  $r2$  and  $r4$  sweep to achieve axial ratio.

Moreover, when  $r1$ ,  $r2$ ,  $r3$ , and  $r4$  are not designed in the decreasing size order, as required in Section II, the axial ratio deteriorates and can be seen for the two cases, presented in the Figure 5.

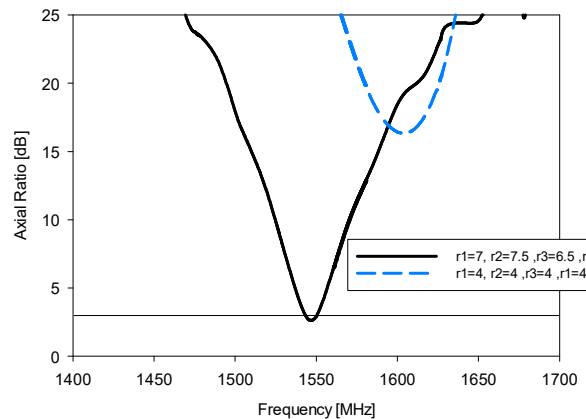


Fig.5 Ring slots radii when not taken in the desired order

To validate the circular polarization characteristic of the antenna, AR results is necessary[16]. The AR of less than 3 dB is sufficient to ensure the antenna is circularly polarized.

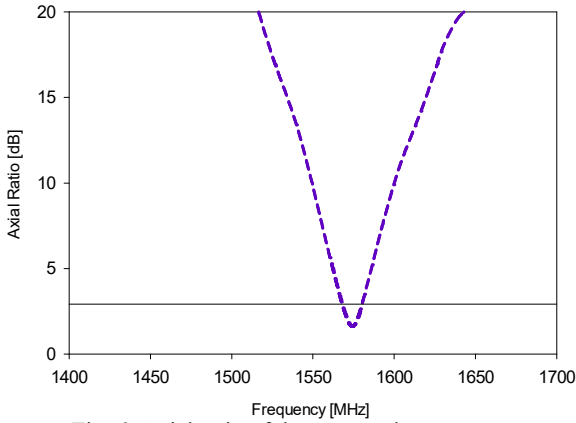


Fig. 6. Axial ratio of the proposed antenna

Figure 6 represents the axial ratio plot, where the axial ratio is less than 3 dB with a bandwidth of 14.13 MHz at 1575 MHz. Radiation patterns for the proposed antenna is illustrated in Figure 7. The boresight realized gain is 5.58 dB with a 3-dB angular width of 96.6° at  $\phi = 0^\circ$ , and 97.3° at  $\phi = 90^\circ$ .

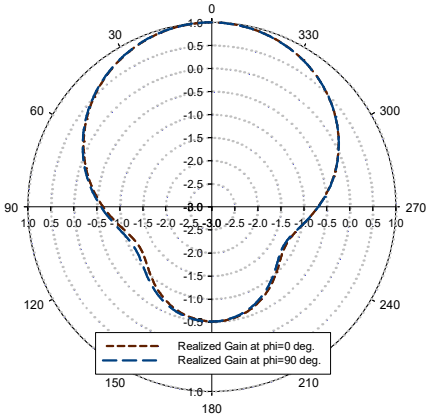


Fig. 7. Far-field realized gain at 1575 MHz for  $\phi = 0^\circ$  and  $\phi = 90^\circ$

Figure 8 illustrates that the antenna is right hand circular polarized, with a forward gain of 5.46 dB in the forward direction at  $\theta = 0^\circ$ . Besides that, the opposite polarization at  $\theta = 0^\circ$  is -9.67 dB.

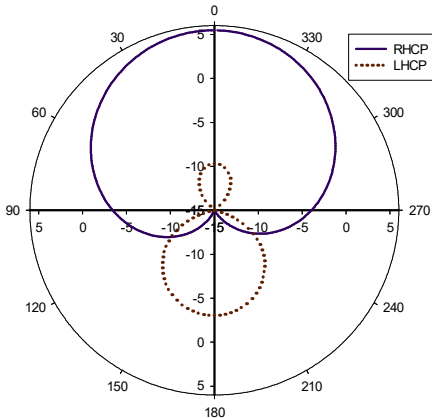


Fig. 8. Radiation pattern at 1575 MHz illustrating RHCP and LHCP

Surface currents on the antenna patch are presented at four different phases with an interval of  $90^\circ$  in Figure 9. In each subfigure, surface current vectors are observed to be mainly rotating in counterclockwise, indicating the antenna's RHCP mode.

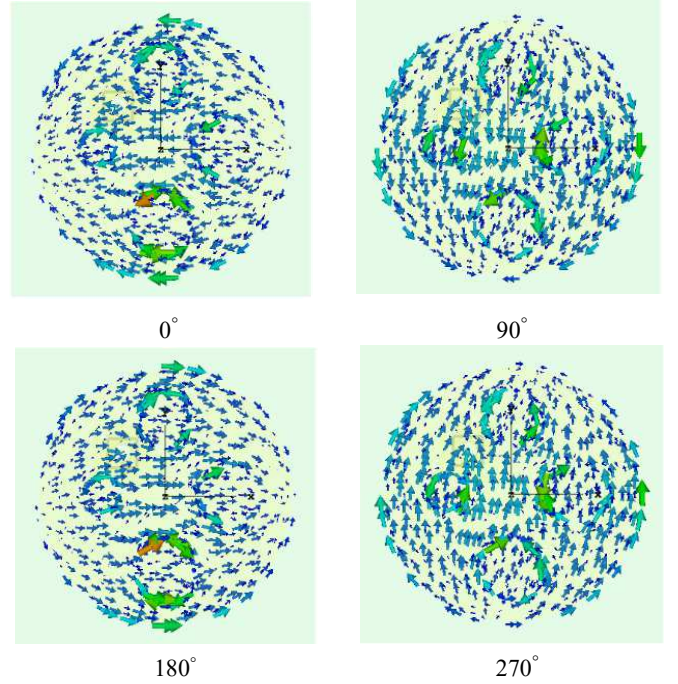


Fig. 9. Current distribution of the proposed antenna operating at 1575 MHz for four different phases.

The proposed antenna is compared in terms of antenna size, gain and bandwidth with existing antenna designs operating at L1 band, as presented in the Table I. It can be seen that this antenna fulfills the requirements of the GNSS receivers and is compact in size with satisfactory gain.

TABLE I  
ANTENNA SPECIFICATIONS COMPARISON TABLE

Ref.	Bandwidth MHz/Fraction	Gain [dB]	Size in $\lambda_o$ (and mm)
[9]	50/3.17%	6.6	$R = 0.289\lambda_o$ (55)
[10]	81/5.14%	3.2	$0.58\lambda_o \times 0.49\lambda_o \times 0.05\lambda_o$ (111×94×10)
[11]	640/40.63%	0.42	$0.43\lambda_o \times 0.47\lambda_o \times 0.004\lambda_o$ (90×82×0.8)
[12]	450/28.57%	Approx. 10	$R = 1.89\lambda_o$ (360)
[13]	500/31.75%	1.6	$0.47\lambda_o \times 0.47\lambda_o \times 0.11\lambda_o$ (89×89×20)
Proposed Design	30.87/1.96%	5.58	$0.34\lambda_o \times 0.34\lambda_o \times 0.02\lambda_o$ (65×66×3.25)

#### IV. CONCLUSION

A compact GNSS circularly polarized antenna operating at L1 band has been designed and presented. Miniaturization of the structure is achieved using four ring slots created on the

radiator. Impedance bandwidth of the antenna is 1.96 %, main lobe direction is facing upward at an angle of 0° and the axial ratio is less than 3 dB at 1575 MHz.

#### REFERENCES

- [1] J. J. H. Wang, "Antennas for global navigation satellite system (GNSS)," *Proc. IEEE*, vol. 100, no. 7, pp. 2349–2355, 2012.
- [2] "GPS L1/L2 Antenna - Helix Technologies." [Online]. Available: <https://helixtechnologies.co.uk/multi-frequency-gnss-antennas-2/gps-l1-l2-antenna/>. [Accessed: 20-Aug-2021].
- [3] C. J. Wang, M. H. Shih, and L. T. Chen, "A wideband open-slot antenna with dual-band circular polarization," *IEEE Antennas Wirel. Propag. Lett.*, vol. 14, no. c, pp. 1306–1309, 2015.
- [4] E. Al Abbas, A. T. Mobashsher, and A. Abbosh, "Polarization reconfigurable antenna for 5G cellular networks operating at millimeter waves," *Asia-Pacific Microw. Conf. Proceedings, APMC*, pp. 772–774, 2017.
- [5] S. Kibria, M. T. Islam, and B. Yatim, "New compact dual-band circularly polarized universal RFID reader antenna using ramped convergence particle swarm optimization," *IEEE Trans. Antennas Propag.*, vol. 62, no. 5, pp. 2795–2801, 2014.
- [6] R. Joshi *et al.*, "Dual-Band, Dual-Sense Textile Antenna with AMC Backing for Localization Using GPS and WBAN/WLAN," *IEEE Access*, vol. 8, pp. 89468–89478, 2020.
- [7] Z. Wang, S. Fang, S. Fu, and S. Lü, "Dual-band probe-fed stacked patch antenna for GNSS applications," *IEEE Antennas Wirel. Propag. Lett.*, vol. 8, pp. 100–103, 2009.
- [8] Y. Sun, K. W. A. Leung, and J. Ren, "Dual-Band Circularly Polarized Antenna With Wide Axial Ratio Beamwidths for Upper Hemispherical Coverage," *IEEE Access*, vol. 6, pp. 58132–58138, 2018.
- [9] P. Yang, F. Yan, L. Zhou, M. Gao, and F. Yang, "A small low-multipath GNSS antenna using annular slot loaded ground plane," *APCAP 2016 - 2016 IEEE 5th Asia-Pacific Conf. Antennas Propagation, Conf. Proc.*, pp. 349–350, 2017.
- [10] M. S. Shakhirul *et al.*, "1.575 GHz Circular Polarization wearable antenna with three different substrate materials," *2014 IEEE Asia-Pacific Conf. Appl. Electromagn. APACE 2014 - Proceeding*, pp. 43–46, 2015.
- [11] Y. F. Cao, S. W. Cheung, L. Liu, and T. I. Yuk, "A simple planar circularly polarized antenna for GPS system," *2014 Int. Work. Antenna Technol. Small Antennas, Nov. EM Struct. Mater. Appl. iWAT 2014*, pp. 355–358, 2014.
- [12] F. Scire-Scappuzzo and S. N. Makarov, "A low-multipath wideband GPS antenna with cutoff or non-cutoff corrugated ground plane," *IEEE Trans. Antennas Propag.*, vol. 57, no. 1, pp. 33–46, 2009.
- [13] J. A. Kasemodel, C. C. Chen, I. J. Gupta, and J. L. Volakis, "Miniature continuous coverage antenna array for GNSS receivers," *IEEE Antennas Wirel. Propag. Lett.*, vol. 7, pp. 592–595, 2008.
- [14] S. I. H. Shah, S. Bashir, and A. Altaf, "Miniaturization of microstrip patch antenna by using various shaped slots for wireless communication systems," *Proc. Int. Semin. Direct Inverse Probl. Electromagn. Acoust. Wave Theory, DIPED*, pp. 92–95, 2014.
- [15] S. Shrestha, S. J. Han, S. K. Noh, S. Kim, H. B. Kim, and D. Y. Choi, "Design of modified Sierpinski fractal based miniaturized patch antenna," *Int. Conf. Inf. Netw.*, pp. 274–279, 2013.
- [16] B. Y. Toh, R. Cahill, and V. F. Fusco, "Understanding and measuring circular polarization," *IEEE Trans. Educ.*, vol. 46, no. 3, pp. 313–318, 2003.